J|A|C|S ARTICLES

Published on Web 03/16/2009

Impact of Metallophilicity on "Colossal" Positive and Negative Thermal Expansion in a Series of Isostructural Dicyanometallate Coordination Polymers

Jasmine L. Korčok, Michael J. Katz, and Daniel B. Leznoff*

Department of Chemistry, Simon Fraser University, 8888 University Dr., Burnaby, BC, Canada V5A 1S6

Received December 9, 2008; E-mail: dleznoff@sfu.ca

Abstract: Five isostructural dicyanometallate coordination polymers containing metallophilic interactions ($In[M(CN)_2]_3$ (M = Ag, Au), $KCd[M(CN)_2]_3$, and $KNi[Au(CN)_2]_3$) were synthesized and investigated by variable-temperature powder X-ray diffraction to probe their thermal expansion properties. The compounds have a trigonal unit cell and show positive thermal expansion (PTE) in the *ab* plane, where Kagome sheets of M atoms reside, and negative thermal expansion (NTE) along the trigonal *c* axis, perpendicular to these sheets. The magnitude of thermal expansion is unusually large in all cases (40×10^{-6} K^{-1} < $|\alpha|$ < 110×10^{-6} K^{-1}). The system with the weakest metallophilic interactions, $In[Ag(CN)_2]_3$, shows the most "colossal" thermal expansion of the series ($\alpha_a = 105(2) \times 10^{-6}$ K^{-1}, $\alpha_c = -84(2) \times 10^{-6}$ K^{-1} at 295 K), while systems containing stronger Au−Au interactions show relatively reduced thermal expansion. Thus, it appears that strong metallophilic interactions hinder colossal thermal expansion behavior. Additionally, the presence of K^+ counterions also reduces the magnitude of thermal expansion.

Introduction

Most materials encountered on a daily basis expand when they are heated; this behavior is known as positive thermal expansion (PTE). Negative thermal expansion (NTE) is the opposite, that is, contraction of volume or length upon heating. NTE compounds have potential applications in composites with PTE compounds for tailoring the thermal expansion of a material, so that it may function in extremely high or low temperatures or remain functional over a wide range of temperatures without degradation.[1] NTE is known for a range of substances such as metal oxides (those with M−O−M′ or O−M−O bridges[2]), metal cyanides (Prussian Blue analogues[3−5] and simple cyanides $M(CN)_x$[6−8]), and even water between 0 and 4 °C. Materials that have anisotropic solid state structures generally show anisotropic thermal expansion.[9] Most commonly, this is positive in all directions, although some examples are known of structures exhibiting PTE coupled with orthogonal NTE, such as in $PbTiO_3$,[10] β-eucryptite,[11] Mg-cordierite,[12] and the NZP (sodium zirconium phosphate)[13] and $A_2M_3O_{12}$[14] families.

Cyanometallate coordination polymers are prime targets for investigating thermal expansion behavior because transverse vibrational motion of the cyanides is known to lead to negative thermal expansion.[6,15] It was recently shown that the silver(I) hexacyanocobaltate(III) and hexacyanoferrate(III) coordination polymers, $Ag_3[Co(CN)_6]$ and $Ag_3[Fe(CN)_6]$, are anisotropic thermal expansion materials: they simultaneously expand along two crystal axes while contracting along the third upon heating, with positive and negative thermal expansion coefficients 10 times greater than those typically observed in solids (dubbed "colossal").[16,17] Gold and silver building blocks are interesting because they can form *metallophilic* d^{10} closed-shell interac-

(1) Evans, J. S. O. *J. Chem. Soc., Dalton Trans.* **1999**, 3317.
(2) (a) Korthuis, V.; Khosrovani, N.; Sleight, A. W.; Roberts, N.; Dupree, R.; Warren, W. W., Jr. *Chem. Mater.* **1995**, *7*, 412. (b) Mary, T. A.; Evans, J. S. O.; Vogt, T.; Sleight, A. W. *Science* **1996**, *272*, 90. (c) Lind, C.; Wilkinson, A. P.; Hu, Z.; Short, S.; Jorgensen, J. D. *Chem. Mater.* **1998**, *10*, 2335. (d) Attfield, M. P.; Sleight, A. W. *Chem. Commun.* **1998**, 601. (e) Attfield, M. P.; Sleight, A. W. *Chem. Mater.* **1998**, *10*, 2013. (f) Woodcock, D. A.; Lightfoot, P.; Villaescusa, L. A.; Días-Cabañas, M.-J.; Camblor, M. A.; Engberg, D. *Chem. Mater.* **1999**, *11*, 2508. (g) Lightfoot, P.; Woodcock, D. A.; Maple, M. J.; Villaescusa, L. A.; Wright, P. A. *J. Mater. Chem.* **2001**, *11*, 212. (h) Li, J.; Yokochi, A.; Amos, T. G.; Sleight, A. W. *Chem. Mater.* **2002**, *14*, 2602. (i) Tiano, W.; Dapiaggi, M.; Artioli, G. *J. Appl. Crystallogr.* **2003**, *36*, 1461.
(3) (a) Margadonna, S.; Prassides, K.; Fitch, A. N. *J. Am. Chem. Soc.* **2004**, *126*, 15390. (b) Pretsch, T.; Chapman, K. W.; Halder, G. J.; Kepert, C. J. *Chem. Commun.* **2006**, 1857.
(4) Goodwin, A. L.; Chapman, K. W.; Kepert, C. J. *J. Am. Chem. Soc.* **2005**, *127*, 17980.
(5) Chapman, K. W.; Chupas, P. J.; Kepert, C. J. *J. Am. Chem. Soc.* **2006**, *128*, 7009.
(6) Goodwin, A. L.; Kepert, C. J. *Phys. Rev. B* **2005**, *71*, 140301.
(7) (a) Hibble, S. J.; Hannon, A. C.; Cheyne, S. M. *Inorg. Chem.* **2003**, *42*, 4724. (b) Reckeweg, O.; Lind, C.; Simon, A.; DiSalvo, F. J. *Z. Naturforsch.* **2003**, *58b*, 155.
(8) Hibble, S. J.; Chippindale, A. M.; Pohl, A. H.; Hannon, A. C. *Angew. Chem., Int. Ed.* **2007**, *46*, 7116.
(9) Sleight, A. W. *Endeavour* **1995**, *19*, 64.
(10) Shirane, G.; Hoshino, S. *J. Phys. Soc. Jpn.* **1951**, *6*, 265.
(11) Gillery, F. H.; Bush, E. A. *J. Am. Ceram. Soc.* **1959**, *42*, 175.
(12) Hochella, M. F., Jr.; Brown, G. E.; Ross, F. K.; Gibbs, G. V. *Am. Mineral.* **1979**, *64*, 337.
(13) Oota, T.; Yamai, I. *J. Am. Ceram. Soc.* **1986**, *69*, 1.
(14) Evans, J. S. O.; Mary, T. A.; Sleight, A. W. *J. Solid State Chem.* **1997**, *133*, 580.
(15) Chapman, K. W.; Chupas, P. J.; Kepert, C. J. *J. Am. Chem. Soc.* **2005**, *127*, 15630.
(16) Goodwin, A. L.; Calleja, M.; Conterio, M. J.; Dove, M. T.; Evans, J. S. O.; Keen, D. A.; Peters, L.; Tucker, M. G. *Science* **2008**, *319*, 794.

10.1021/ja809631r CCC: $40.75 © **2009 American Chemical Society**

tions;[18] these interactions have been exploited for luminescent, sensing, conductive, birefringent and other functional properties.[19] Weak argentophilic interactions were postulated to drive the colossal behavior in $Ag_3[Co(CN)_6]$ and $Ag_3[Fe(CN)_6]$,[16,17,20,21] but the effects of metallophilicity on thermal expansion behavior have otherwise been virtually unexplored. In order to probe this in a systematic fashion, we prepared a series of new $[Au(CN)_2^-]$- and $[Ag(CN)_2^-]$-based coordination polymers that have the same trigonal structure as $Ag_3[Co(CN)_6]$ and $Ag_3[Fe(CN)_6]$ and herein report on their large anisotropic thermal expansion.

Experimental Section

General Procedures and Physical Characterizations. All reagents were obtained from commercial suppliers and used as received. All manipulations were performed in air. Infrared spectra were obtained as KBr pellets on a Thermo Nicolet Nexus FTIR spectrometer with a 1 cm^{-1} resolution. Fluorescence spectra were recorded on a Photon Technology International QuantaMaster UV−vis spectrofluorometer. Elemental analyses (C, H, N) were performed by Mr. Farzad Haftbaradaran at Simon Fraser University using a computer-controlled Carlo Erba (Model 1110) CHN analyzer. Thermogravimetric analyses were performed on a Shimadzu TGA-50 using a heating rate of 5 °C/min up to 600 °C. Porosity measurements were carried out on a Micromeritics ASAP 2020 porosimeter. N_2 adsorption/desorption isotherms were collected on degassed samples at 77 K in the pressure range 5−750 mmHg $N_{2(g)}$.

Synthesis of $In[Au(CN)_2]_3$. An acidified aqueous solution (pH 2.45) of $KAu(CN)_2$ (65 mg; 0.23 mmol in 2 mL) was added to an acidified aqueous solution of $InCl_3 \cdot 3H_2O$ (25 mg; 0.090 mmol in 2 mL). After 2 h a very pale yellow powder of $In[Au(CN)_2]_3$ was filtered, washed with water, and air-dried. Yield = 32% (21 mg; 0.024 mmol). IR: 2184 (vs; ν_{CN}), 2145 (w; $\nu^{13}{}_{CN}$), 995 (vw, br), 498 cm^{-1} (m). Fluorimetry: $\lambda_{ex} = 375$ nm, $\lambda_{em} = 410$ and 495 nm. Anal. Calcd for $C_6N_6Au_3In$: C 8.36%, H 0%, N 9.75%; found: C 8.32%, H 0%, N 9.82%.

Synthesis of $In[Ag(CN)_2]_3 \cdot xH_2O$. An aqueous solution of $KAg(CN)_2$ (92 mg; 0.46 mmol in 2 mL) was added to an aqueous solution of $InCl_3 \cdot 3H_2O$ (48 mg; 0.17 mmol in 2 mL). An immediate white precipitate was obtained (80 mg). A small and variable amount (<10%) of coprecipitated, insoluble AgCN is formed in the reaction regardless of concentrations or indium salt used, detected by a shoulder peak at 2166 cm^{-1} in the IR and confirmed by a powder pattern. As a result, a clean elemental analysis could not be obtained. $In[Ag(CN)_2]_3(\cdot xH_2O)$ is light sensitive. IR: 2186 (vs; ν_{CN}), 2141 (w; $\nu^{13}{}_{CN}$), 477 cm^{-1} (m).

Synthesis of $KCd[Au(CN)_2]_3$. Slow evaporation of an aqueous solution of $KAu(CN)_2$ (99 mg; 0.34 mmol in 15 mL) and $Cd(NO_3)_2 \cdot 4H_2O$ (38 mg; 0.12 mmol in 15 mL) yielded thin, colorless plates of $KCd[Au(CN)_2]_3$ after about 3 weeks (58%; 59 mg; 0.066 mmol). IR: 2158 (vs; ν_{CN}), 2119 (w; $\nu^{13}{}_{CN}$), 730 (w, br), 455 cm^{-1} (m). Fluorimetry: $\lambda_{ex} = 386$ nm, $\lambda_{em} = 455$ nm. Anal. Calcd for $C_6N_6Au_3CdK$: C 8.02%, H 0%, N 9.35%; found: C 7.93%, H 0%, N 9.65%.

Synthesis of $KCd[Ag(CN)_2]_3$. An aqueous solution of $KAg(CN)_2$ (207 mg; 1.04 mmol in 15 mL) was added to an aqueous solution of $Cd(NO_3)_2 \cdot 4H_2O$ (115 mg; 0.372 mmol in 15 mL). Thin, colorless plates of $KCd[Ag(CN)_2]_3$ were obtained after approximately an hour (52.1%; 114 mg; 0.181 mmol). $KCd[Ag(CN)_2]_3$ is light sensitive, so was crystallized under a foil pyramid. IR: 2158 (vs; ν_{CN}), 2114 (w; $\nu^{13}{}_{CN}$), 419 cm^{-1} (vs). Fluorimetry: $\lambda_{ex} = 277$ and 297 nm, $\lambda_{em} = 340$ nm. Anal. Calcd for $C_6N_6Ag_3CdK$: C 11.42%, H 0%, N 13.31%; found: C 11.38%, H 0%, N 13.41%.

Powder X-ray Crystallographic Analysis. Variable-temperature powder X-ray diffraction experiments were performed on a Bruker SMART diffractometer equipped with an APEX II CCD detector and a Mo Kα fine focus sealed X-ray tube ($\lambda = 0.71073$ nm) operated at 1.5 kW (50 kV, 30 mA) and filtered with a graphite monochromator. Samples were ground and sealed in a glass capillary; $In[Ag(CN)_2]_3 \cdot xH_2O$ was also run in an open capillary. Twenty measurements were obtained while ramping the temperature down from 395 to 100 K (and also up from 100 to 395 K) in ~15 K steps using an Oxford Cryosystems Cryostream. Data were collected by a spinning ϕ scan at 360° over the ranges $1° \le 2\theta \le 26°$ and $12° \le 2\theta \le 37°$ (to constitute the full 2θ range of $1° \le 2\theta \le 37°$) at each temperature with 300 s exposure times. Powder patterns were simulated and refined using standard Rietveld methods in the program PowderCell (v. 2.4);[22] peaks were fit using Gaussian lineshapes at all temperatures. A sample powder pattern simulation for $In[Au(CN)_2]_3$ is given in Figure S1.

Single-Crystal X-ray Crystallographic Analysis. All measurements were collected on a Bruker SMART diffractometer equipped with an APEX II CCD detector and a Mo Kα fine focus sealed X-ray tube ($\lambda = 0.71073$ nm) operated at 1.5 kW (50 kV, 30 mA) and filtered with a graphite monochromator. A colorless platelet of $KCd[Au(CN)_2]_3$ of dimensions $0.022 \times 0.133 \times 0.180$ mm^3 was mounted on a glass fiber with epoxy adhesive. Variable temperatures were achieved using an Oxford Cryosystems Cryostream. Data were collected between $5° \le 2\theta \le 75°$ by ω and ϕ scans (scan width = 0.5°) using 5.0 s exposure times. The structures were solved using direct methods (SIR 92) and refined by least-squares procedures in CRYSTALS.[23]

Results and Discussion

The four structurally analogous coordination polymers $In[Ag(CN)_2]_3 \cdot xH_2O$, $In[Au(CN)_2]_3$, $KCd[Ag(CN)_2]_3$, and $KCd[Au(CN)_2]_3$ were synthesized by addition of stoichiometric amounts of aqueous $KM(CN)_2$ (M = Ag, Au) to aqueous $InCl_3$ or $Cd(NO_3)_2$. Single-crystal X-ray diffraction studies were performed on $KCd[Au(CN)_2]_3$ (see Table 1 for crystallographic data) and although single crystals of $In[M(CN)_2]_3$ could not be obtained, powder diffractograms indicated that all polymers were isostructural (Table 2) and the $In[M(CN)_2]_3$ structures were refined on the basis of the atomic coordinates of $KCd[Au(CN)_2]_3$. The recently reported $KNi[Au(CN)_2]_3$ is also isostructural.[24] All five systems have similar trigonal unit cells: $P312$ for the compounds with potassium, and in the absence of any single crystal data, $In[M(CN)_2]_3$ were modeled in the centrosymmetric equivalent $P\bar{3}1m$. The complexes feature pseudo-octahedrally coordinated indium(III), cadmium(II), or nickel(II) metal sites, linked by six $Au(CN)_2^-$ or $Ag(CN)_2^-$

(17) Goodwin, A. L.; Keen, D. A.; Tucker, M. G.; Dove, M. T.; Peters, L.; Evans, J. S. O. *J. Am. Chem. Soc.* **2008**, *130*, 9660.
(18) (a) Schmidbaur, H. *Chem. Soc. Rev.* **1995**, *24*, 391. (b) Pyykkö, P. *Chem. Rev.* **1997**, *97*, 597. (c) Pyykkö, P. *Angew. Chem., Int. Ed.* **2004**, *43*, 4412.
(19) (a) Yam, V. W.-W.; Li, C.-K.; Chan, C.-L. *Angew. Chem., Int. Ed.* **1998**, *37*, 2857. (b) Rawashdeh-Omary, M. A.; Omary, M. A.; Patterson, H. H.; Fackler, J. P., Jr. *J. Am. Chem. Soc.* **2001**, *123*, 11237. (c) Lefebvre, J.; Batchelor, R. J.; Leznoff, D. B. *J. Am. Chem. Soc.* **2004**, *126*, 16117. (d) White-Morris, R. L.; Olmstead, M. M.; Attar, S.; Balch, A. L. *Inorg. Chem.* **2005**, *44*, 5021. (e) Katz, M. J.; Ramnial, T.; Yu, H.-Z.; Leznoff, D. B. *J. Am. Chem. Soc.* **2008**, *130*, 10662. (f) Rao, C. N. R.; Ranganathan, A.; Pedireddi, V. R.; Raju, A. R. *Chem. Commun.* **2000**, 39. (g) Katz, M. J.; Kaluarachchi, H.; Batchelor, R. J.; Bokov, A. A.; Ye, Z.-G.; Leznoff, D. B. *Angew. Chem., Int. Ed.* **2007**, *46*, 8804.
(20) Conterio, M. J.; Goodwin, A. L.; Tucker, M. G.; Keen, D. A.; Dove, M. T.; Peters, L.; Evans, J. S. O. *J. Phys: Condens. Matter* **2008**, *20*, 255225.
(21) Calleja, M.; Goodwin, A. L.; Dove, M. T. *J. Phys: Condens. Matter* **2008**, *20*, 255226.
(22) Kraus, W.; Nolze, N. *J. Appl. Crystallogr.* **1996**, *29*, 301.
(23) Betteridge, P. W.; Carruthers, J. R.; Cooper, R. I.; Prout, K.; Watkin, D. J. *J. Appl. Crystallogr.* **2003**, *36*, 1487.
(24) Lefebvre, J.; Trudel, S.; Hill, R. H.; Leznoff, D. B. *Chem. Eur. J.* **2008**, *14*, 7156.

Table 1. Crystallographic Data for $KCd[Au(CN)_2]_3$

empirical formula	$C_6N_6Au_3CdK$			
formula weight	898.51			
crystal color	colorless			
crystal system	hexagonal			
space group	$P\bar{3}12$			
Z	1			
temperature (K)	100	205	295	395
a (Å)	6.76520(10)	6.81070(10)	6.8576(2)	6.9098(2)
c (Å)	8.3094(4)	8.2665(3)	8.2251(4)	8.1724(4)
V (Å^3)	329.353(17)	332.075(14)	334.98(2)	337.92(2)
ρ_{calcd} (g cm^{-1})	4.530	4.493	4.454	4.415
μ (mm^{-1})	35.195	34.907	34.604	34.303
reflns ($I > 2.5\sigma(I)$)	873	780	730	567
R (F_o)	0.0183	0.0169	0.0180	0.0219
R_w (F_o)	0.0194	0.0156	0.0193	0.0233
GOF	0.470	0.457	0.433	0.530

Table 2. Unit Cell Parameters for $In[M(CN)_2]_3(\cdot xH_2O)$, $KCd[Ag(CN)_2]_3$, and $KNi[Au(CN)_2]_3$ Obtained from Powder X-ray Diffraction at Room Temperature (295 K)

empirical formula	$C_6N_6Au_3In$	$C_6N_6Ag_3In$	$C_6N_6Ag_3In(H_2O)_x$	$C_6N_6Ag_3CdK$	$C_6N_6Au_3KNi$[a]
crystal system	hexagonal	hexagonal	hexagonal	hexagonal	hexagonal
space group	$P\bar{3}1m$	$P\bar{3}1m$	$P\bar{3}1m$	$P312$	$P312$
a (Å)	6.6272(8)	6.9132(14)	6.9060(17)	6.9417(5)	6.786(4)
c (Å)	8.0427(14)	7.9950(14)	8.0171(17)	8.3192(8)	7.778(8)
V (Å^3)	305.91(6)	330.91(15)	331.13(16)	347.17(3)	310.2(4)

[a] Reference 24, single-crystal data.

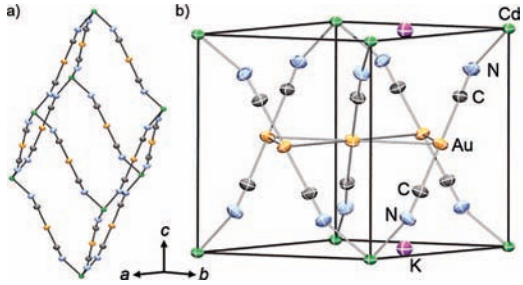

Figure 1. (a) Distorted cubic framework of $KCd[Au(CN)_2]_3$ (K atoms omitted for clarity). Green = Cd; gold = Au; gray = C; blue = N. (b) Unit cell of $KCd[Au(CN)_2]_3$ (295 K). Thermal ellipsoids are shown at 50% probability. $In[M(CN)_2]_3$ structures are without K atoms.

bridging units to form a distorted cubic Prussian Blue-type framework (Figure 1a). There are three interpenetrated networks that make up the overall structure. With respect to the unit cell (Figure 1b), In, Cd, or Ni atoms lie on the corners, creating planes of metal atoms in the *ab* plane. Between these are planes of gold or silver atoms at *c*/2, arranged in a Kagome lattice.[25] Metals in adjacent planes are linked by cyanides running roughly parallel to the {101} planes. Where a potassium counterion is present, K^+ lies on a 3-fold axis in the (001) plane (Figure 1b). These compounds are isostructural to $Ag_3[Co(CN)_6]$ and $Ag_3[Fe(CN)_6]$ (space group $P\bar{3}1m$), recently reported to show "colossal" PTE and NTE, but in the polymers reported here the Au and Ag atoms are C-bound to the cyanides, whereas in $Ag_3[M(CN)_6]$ (M = Co^{III}, Fe^{III}) the Ag atoms are N-bound (confirmed by neutron diffraction). In general, it can be difficult to distinguish between C and N by X-ray diffraction and modeling C/N disorder is often required, but in this case, single-crystal studies of $KCd[Au(CN)_2]_3$ and $KNi[Au(CN)_2]_3$[24] unambiguously showed that the Au atoms are C-bound to the cyanides without structural disorder. This basic structural motif has also

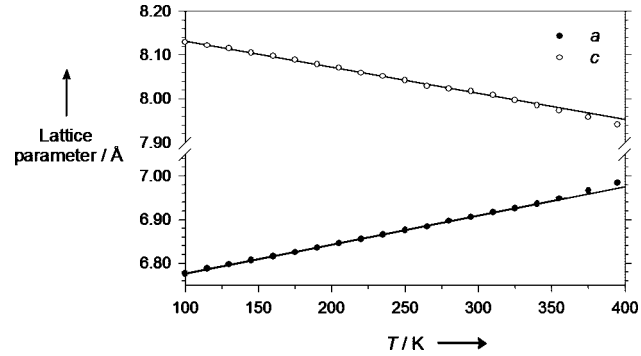

Figure 2. Change in lattice parameters (Å) in $In[Ag(CN)_2]_3\cdot xH_2O$ as a function of temperature (K). Closed circles, *a*; open circles, *c*. Dehydration begins around 340 K. Errors are within the points.

been observed in $Ln[M(CN)_2]_3(H_2O)_3$ (Ln = Tb, Gd, Y, La; M = Ag, Au),[26] $KCo[Au(CN)_2]_3$,[27] $KFe[Au(CN)_2]_3$,[28] $KMn[Ag(CN)_2]_3(H_2O)$,[29] and $RbCd[Ag(CN)_2]_3$.[30]

A series of powder X-ray diffraction experiments was performed on the compounds between 100 and 395 K to determine how the unit cell changes with temperature. All compounds show immense anisotropic thermal expansion: they expand in the *ab* plane and contract along the *c* direction upon heating, in the same manner as $Ag_3[Co(CN)_6]$ and $Ag_3[Fe(CN)_6]$. This corresponds to PTE in the planes of the metal atoms, and NTE perpendicular to these planes. A plot of the change in lattice parameters as a function of temperature is shown in Figure 2 for $In[Ag(CN)_2]_3\cdot xH_2O$ (see Figures S2−S6 for the analogous plots for $In[M(CN)_2]_3$, $KCd[M(CN)_2]_3$, and $KNi[Au(CN)_2]_3$). The magnitude of the change is expressed by the thermal expansion coefficient α (Table 3), which is defined here as $\alpha_l = d(\ln l)/dT$. All polymers display approximately linear thermal expansion behavior, and no appreciable hysteresis was observed whether warming or cooling the samples. The thermal expansion for most of the compounds is not considered "colossal" by the definition given by Goodwin et al. ($|\alpha_l| > 100 \times 10^{-6}$ K^{-1}),[16] but they all display very large NTE and PTE. This series of measurements confirms that the concept of colossal thermal expansion can be generalized to Prussian Blue analogues containing $d^{10}-d^{10}$ metallophilic interactions and thus should be observable in other related systems.

Uniquely, $In[Ag(CN)_2]_3\cdot xH_2O$ was isolated as a hydrate, as confirmed by thermogravimetric analysis; dehydration occurs between 343 and 368 K (4.0% mass loss observed, corresponding to $x \approx 1.4$ H_2O). Upon heating the hydrate from 100 K to obtain the unit cell parameters, the magnitude of the slope $|dl/dT|$ increased rapidly around 340 K, consistent with dehydration (Figure 2). Upon cooling the dehydrated $In[Ag(CN)_2]_3$ from 395 K, it displayed larger α_l values than the hydrated analogue. This phenomenon has been observed in other desorbed host/guest structures.[31] Below 190 K, the slope trailed off slightly,

(25) Syôzi, I. *Prog. Theor. Phys.* **1951**, *6*, 306.

(26) (a) Rawashdeh-Omary, M. A.; Larochelle, C. L.; Patterson, H. H. *Inorg. Chem.* **2000**, *39*, 4527. (b) Colis, J. C. F.; Larochelle, C.; Staples, R.; Herbst-Irmer, R.; Patterson, H. *J. Chem. Soc., Dalton Trans.* **2005**, 675.

(27) Abrahams, S. C.; Bernstein, J. L.; Liminga, R.; Eisenmann, E. T. *J. Phys. Chem.* **1980**, *73*, 4585.

(28) Dong, W.; Zhu, L.-N.; Sun, Y.-Q.; Liang, M.; Liu, Z.-Q.; Liao, D.-Z.; Jiang, Z.-H.; Yan, S.-P.; Cheng, P. *Chem. Commun.* **2003**, 2544.

(29) Dong, W.; Wang, Q.-L.; Si, S.-F.; Liao, D.-Z.; Jiang, Z.-H.; Yan, S.-P.; Cheng, P. *Inorg. Chem. Commun.* **2003**, *6*, 873.

(30) Hoskins, B. F.; Robson, R.; Scarlett, N. V. Y. *Chem. Commun.* **1994**, 2025.

Table 3. Thermal Expansion Coefficients in the *a* Direction, *c* Direction, and along the {101} Planes from 100 to 395 K unless Otherwise Noted[a]

compound	$\alpha_a/\times10^{-6}$ K^{-1}	$\alpha_c/\times10^{-6}$ K^{-1}	$\alpha_{101}/\times10^{-6}$ K^{-1}
$In[Au(CN)_2]_3$	+86.1 to +83.9	−62.2 to −63.3	−4.14 to −2.69
$In[Ag(CN)_2]_3 \cdot xH_2O$[b]	+98 to +95	−73 to −75	−3.33 to −1.75
$In[Ag(CN)_2]_3$[c]	+104 to +106	−85 to −83	−1.97 to −3.58
$KCd[Au(CN)_2]_3$	+72.9 to +71.4	−56.1 to −57.1	−4.60 to −3.41
$KCd[Ag(CN)_2]_3$	+76.6 to + 74.9	−64.3 to −65.6	−8.3 to −6.9
$KNi[Au(CN)_2]_3$	+59.7 to + 58.7	−42.2 to −42.7	+1.79 to +2.53
$Ag_3[Co(CN)_6]$[d]	+144(9)	−126(4)	+4.63[e]
$Ag_3[Fe(CN)_6]$[f]	+124.0(10)	−113(3)	−
$H_3[Co(CN)_6]$[g]	+17.4(6)	−5.04(24)	−

[a] α_l is defined as $\alpha_l = d(\ln l)/dT$. Errors are calculated to be $\sim \pm 1-2\%$. See Supporting Information for α_l values over the entire temperature range with errors. [b] From 100 to 325 K. [c] From 395 to 205 K. [d] Reference 17, mean α_l values between 10 and 300 K. [e] From ref 16, mean value calculated from X-ray data between 16 and 297 K. [f] Reference 17, mean α_l values between 8 and 310 K. [g] Reference 17, mean α_l values between 8 and 304 K.

Table 4. Metal−Metal Distances (Au or Ag) at 100 and 395 K[a,b]

compound	M−M distances at 100 K/Å	M−M distances at 395 K/Å
$In[Au(CN)_2]_3$	3.261(1)	3.342(1)
$In[Ag(CN)_2]_3 \cdot xH_2O$	3.388(1)	n/a
$In[Ag(CN)_2]_3$	3.392(1)	3.492(1)
$KCd[Au(CN)_2]_3$	3.319(1), 3.447(1)	3.377(1), 3.533(1)
$KCd[Ag(CN)_2]_3$	3.360(1), 3.484(1)	3.417(1), 3.581(1)
$KNi[Au(CN)_2]_3$	3.312(1), 3.441(1)	3.354(1), 3.515(1)
$Ag_3[Co(CN)_6]$[c]	3.4147(3)	3.5524(4)
$Ag_3[Fe(CN)_6]$[d]	3.4091(7)	−

[a] The $KM'[M(CN)_2]_3$ structures have two inequivalent M-M distances in the acentric $P312$ space group; in the centrosymmetric $P\bar{3}1m$ space group, the $In[M(CN)_2]_3$ structures have only one M−M distance of $a/2$. [b] The longer distances in the acentric structures correspond to those surrounding the K^+ atoms above and below in the *c* direction. [c] From ref 16. [d] From ref 17.

attributed to a small amount of nitrogen sorption from the cryostream.[32] The α_l values for both $In[Ag(CN)_2]_3$ and $In[Ag(CN)_2]_3 \cdot xH_2O$ were obtained from fitting only the region where the data are constant (Table 3).

The d^{10} metal−metal distances for the polymers at the high and low temperature limits probed are listed in Table 4. The accepted maximum distance for a metallophilic interaction is considered to be 3.6 Å for gold[18] and 3.44 Å for silver[33] (the sum of the van der Waals radii); most of the compounds therefore display moderate metal−metal interactions throughout most of the temperature range, with $In[Ag(CN)_2]_3$ displaying virtually no Ag−Ag interactions. Only $In[Au(CN)_2]_3$ and $KCd[M(CN)_2]_3$ show room temperature emission, suggesting that there is metallophilicity in these systems.[26,34]

A few trends can be observed in the data (Table 3). First, both gold-containing compounds show smaller thermal expansion than the silver analogues; this behavior is especially pronounced in $In[M(CN)_2]_3$. In all cases, the Au−Au distances are well within the van der Waals limit and are indeed shorter than the Ag−Ag distances (which are nearly out of the van der Waals range) in the isomorphous Ag analogues. Hence in the $Au(CN)_2^-$ polymers, there are stronger bonding interactions between the M′−NC−Au−CN−M′ (M′ = In, Cd, or Ni) chains of different networks, limiting framework flexibility which leads to less pronounced thermal expansion than in the $Ag(CN)_2^-$ polymers. The flexibility of these linkages is thought to be crucial in thermal expansion behavior.[16,20,21] On the other hand, in $In[Ag(CN)_2]_3$, the long Ag−Ag distances indicate a lack of significant argentophilicity, and it is this structure that shows the largest PTE and NTE of the series. In $Ag_3[Fe(CN)_6]$, the Ag−Ag distances are even longer (Table 4) and it shows even greater PTE and NTE; $Ag_3[Co(CN)_6]$ shows the most colossal PTE and NTE with the longest Ag−Ag distances (Table 4). These results collectively suggest that strong metallophilic interactions hinder thermal expansion in these systems.[35] In the case of the structural analogue $H_3[Co(CN)_6]$, which contains no metal−metal interactions, the thermal expansion is nevertheless much smaller than that observed here (Table 3),[17,36] indicating that the d^{10} metals still play an important role[16,17,20,21] whether they engage in metallophilic bonding or not. However, the strong hydrogen bonding in $H_3[Co(CN)_6]$ (indicated by the short N−H−N distance of 2.60 Å[37] and a broad absorption between 1900 and 600 cm^{-1} in the IR[38]) may hinder the flexibility *within* the Co−CN−H−NC−Co chains required for colossal PTE and NTE.[39]

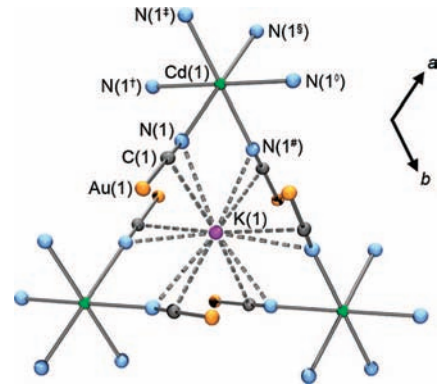

Figure 3. K^+ ions are octahedrally coordinated by six cyanide groups in a side-on fashion in $KCd[M(CN)_2]_3$ and $KNi[Au(CN)_2]_3$.

Second, both indium compounds show greater thermal expansion than the cadmium analogues due to the extra potassium counterions in the latter which can restrict framework motion. All K^+ ions are pseudo-octahedrally surrounded by six cyanide groups coordinated in a side-on fashion (Figure 3), and all CN^- groups have one K^+ ion nearby. The K−C and K−N distances are in the range of those observed in other cyanometallate structures containing side-on coordination of K^+ to CN^-.[40] Any transverse vibrational motion of the cyanides is hindered by the K^+ cations; therefore, less expansion and

(31) Phillips, A. E.; Goodwin, A. L.; Halder, G. J.; Southon, P. D.; Kepert, C. J. *Angew. Chem., Int. Ed.* **2008**, *47*, 1396.
(32) Porosity measurements on the compounds showed that only $In[Ag(CN)_2]_3$ adsorbs a small quantity of nitrogen gas at 77 K.
(33) Bondi, A. *J. Phys. Chem.* **1964**, *68*, 441.
(34) (a) Nagasundaram, N.; Roper, G.; Biscoe, J.; Chai, J. W.; Patterson, H. H.; Blom, N.; Ludi, A. *Inorg. Chem.* **1986**, *25*, 2947. (b) Fischer, P.; Ludi, A.; Patterson, H. H.; Hewat, A. W. *Inorg. Chem.* **1994**, *33*, 62.
(35) The cationic radius of Ag(I) is slightly larger than Au(I), and the larger silver lattices should show greater PTE and NTE than gold since a correlation between thermal expansion and lattice size is expected (for example, see ref 5). However, this effect alone does not account for the differences in the α_l magnitudes observed.
(36) (a) Güdel, H. U.; Ludi, A.; Fischer, P.; Hälg, W. *J. Chem. Phys.* **1970**, *53*, 1917. (b) Güdel, H. U.; Ludi, A.; Fischer, P. *J. Chem. Phys.* **1972**, *56*, 674.
(37) Pauling, L.; Pauling, P. *Proc. Natl. Acad. Sci. U.S.A.* **1968**, *60*, 362.
(38) (a) Jones, D.; Evans, D. F. *Nature* **1963**, *199*, 277. (b) Evans, D. F.; Jones, D.; Wilkinson, G. *J. Chem. Soc.* **1964**, 3164.
(39) Since the polymers reported here have the gold and silver atoms C-bound to the cyanides, this may also serve to hinder flexibility in these systems, given the strength of Au/Ag−C bonds.

Table 5. Bond Lengths and Angles in $KCd[Au(CN)_2]_3$, Obtained from Single-Crystal X-ray Diffraction Data at Four Different Temperatures

bond length/Å	100 K	205 K	295 K	395 K
Cd1−N1	2.331(4)	2.328(3)	2.326(4)	2.341(6)
Au1−Au1[a]	3.3185(9)	3.3373(9)	3.3556(8)	3.3765(14)
Au1−Au1[b]	3.4467(9)	3.4734(9)	3.5020(8)	3.5333(14)
Au1−C1	1.994(4)	1.995(4)	1.994(5)	1.986(7)
C1−N1	1.144(5)	1.141(5)	1.140(6)	1.127(9)
Cd···Cd	10.7151(3)	10.7108(3)	10.7088(4)	10.7020(4)
bond angle/deg	**100 K**	**205 K**	**295 K**	**395 K**
C1−Au1−C1[c]	178.9(7)	178.9(6)	179.4(7)	179.3(11)
Cd1−N1−C1	157.0(3)	157.5(3)	157.9(4)	158.1(7)
N1−C1−Au1	179.1(7)	178.5(8)	177.9(9)	178.1(15)
N1−Cd1−N1[d]	93.2(4)	93.4(4)	93.0(4)	92.7(7)
N1−Cd1−N1[e/f]	86.93(13)	87.12(12)	87.30(15)	87.5(2)
N1−Cd1−N1[g]	92.9(4)	92.4(4)	92.4(4)	92.2(7)
N1−Cd1−N1[h]	179.8(5)	179.3(5)	179.6(5)	179.6(9)

Symmetry transformations: [a] $(-y-1, x-y, z)$. [b] $(-y, x-y+1, z)$. [c] $(-x+y-1, y, -z-1)$. [d] $(x, x-y, -z)$. [e] $(-y, x-y, z)$. [f] $(-x+y, -x, z)$. [g] $(-y, -x, -z)$. [h] $(-x+y, y, -z)$.

contraction is seen in the cadmium (and nickel) compounds. It has been observed in other cyanide frameworks that guests or other interpenetrating networks can hamper (negative) thermal expansion.[4,31]

Finally, comparison of $KNi[Au(CN)_2]_3$ and $KCd[Au(CN)_2]_3$ shows that the α_l values of the latter are significantly larger (Table 3). In addition to slightly longer Au−Au distances in $KCd[Au(CN)_2]_3$, the structure also has a larger lattice than $KNi[Au(CN)_2]_3$ to accommodate the larger Cd^{II} cation, and thus displays correspondingly greater PTE and NTE.[5] Also, α_l could relate to the strength of the M^{II}−N bonds, as observed in related systems;[5] Ni−N is stronger than Cd−N and therefore the structure should be more stiff.

In order to probe the mechanism of thermal expansion, variable-temperature single-crystal studies were performed on $KCd[Au(CN)_2]_3$ at 100, 205, 295, and 395 K (see Table 1 for crystallographic data and Table 5 for bond lengths and angles). No structural phase changes were observed in this range. The thermal expansion coefficients ($\alpha_a = +72.9(3) \times 10^{-6}$ K^{-1}; $\alpha_c = -55.8(3) \times 10^{-6}$ K^{-1} at 100 K) are consistent with those from the powder studies. There are two different Au−Au distances since the Au atoms are not centered at *a*/2 in the acentric structure. The distances are both still within the sum of the van der Waals radii and scale linearly with temperature. Between 100 and 295 K, the C−N, Au−C, and Cd−N distances do not change (within ±1 esd) but do vary from those at 395 K (as expected since thermal motion is more important at higher temperatures); there is an apparent decrease in C−N and Au−C bond lengths at 395 K. However, a Bragg analysis of X-ray diffraction data only provides average bond lengths and angles; a total scattering approach that probes the local structure (for example, see refs 15 or 20) would be complementary to the data provided here and allow for a more detailed mechanistic description, but is beyond the scope of this paper. The anisotropic temperature factors of the cyanides at higher temperatures indicate that motion perpendicular to the Au−C−N chain is greater than that parallel to it. These observations are consistent with transverse motion of the C and N atoms. The NTE behavior may therefore be partly mediated by local transverse vibrations, consistent with what was observed for $Ag_3[Co(CN)_6]$.[16,20]

As the temperature increases, the Cd···Cd distance decreases slightly (Table 5). Thus, the Cd−NC−Au−CN−Cd chains fold slightly with heating, consistent with trends in the crystallographic data indicating that the Cd−N−C angle increases upon heating and N−C−Au decreases. This folding was also observed in $Ag_3[Co(CN)_6]$.[20] In that compound, the PTE and NTE were thought to be coupled by virtue of strong bonding in the Co−CN−Ag−NC−Co linkages; an expansion in the *ab* plane must correspond to a contraction along the *c* axis (and vice versa) in order to maintain the structural integrity of the linkages. This was confirmed by a near-zero thermal expansion coefficient along {101}.[16] The current results support that hypothesis, as the values of α_{101} (Table 3) are all very small relative to α_a and α_c. Thus, the contraction along *c* (NTE) is partially mediated by transverse motion of the cyanides, as well as folding of the Cd−NC−Au−CN−Cd linkages. The expansion in *ab* (PTE) can be rationalized on the basis of anharmonic lattice modes of the d^{10} metal atoms; as the temperature is increased, higher energy metal−metal vibrational (phonon) modes are populated, leading to an increase in average metal−metal bond distance. This rationale is supported by calculations on $Ag_3[Co(CN)_6]$ showing that phonon modes involving displacements of Ag atoms contributed most strongly to the positive Grüneisen parameter γ (a positive γ indicates PTE).[16] It would therefore be expected that weak argentophilic bonds having shallower potential wells (compared to their stronger aurophilic analogues) would generate a larger anharmonic interaction, consistent with the large PTE observed. This would also partly justify why this class of polymers exhibits "colossal" thermal expansion behavior, since metallophilic interactions are weak compared to covalent bonds and therefore should have very low-energy vibrational excited states with significant anharmonicity.

Although not investigated specifically for their thermal expansion behavior, it is worth noting that several polymeric d^{10} Au, Ag, and Cu cyanides (AuCN, CuCN, $KAu(CN)_2$, $TlAu(CN)_2$, and $K_2Na[Ag(CN)_2]_3$) with and without metallophilic interactions display qualitatively similar behavior—expansion in the metal−metal planes with heating and contraction perpendicular to them.[7,34,41] Using existing data from variable temperature structural studies of these polymers, we calculated that they have moderate to large $|\alpha_l|$ values (up to $|80| \times 10^{-6}$ K^{-1}).

Conclusion

The dicyanometallate coordination polymers presented here have shown that highly flexible cyanometallate structures containing d^{10}−d^{10} metallophilic interactions exhibit very large, anisotropic PTE and NTE, thereby supporting the concept of colossal thermal expansion in solid materials. However, increasing the metallophilic interaction strength appears to reduce the colossal thermal expansion behavior: Au−Au bonds are stronger than Ag−Ag analogues, and hence $[Au(CN)_2^-]$-based polymers show correspondingly less PTE and NTE than $[Ag(CN)_2^-]$-based polymers because the networks are more tightly held together. Additionally, the potassium counterions in $KCd[M(CN)_2]_3$ and $KNi[Au(CN)_2]_3$ reduce the thermal expansion

(40) (a) Contakes, S. M.; Rauchfuss, T. B. *Angew. Chem., Int. Ed.* **2000**, *39*, 1984. (b) Adams, H.; Alsindi, W. Z.; Davies, G. M.; Duriska, M. B.; Easun, T. L.; Fenton, H. E.; Herrera, J.-M.; George, M. W.; Ronayne, K. L.; Sun, X.-Z.; Towrie, M.; Ward, M. D. *Dalton Trans.* **2006**, 39.

(41) Fischer, P.; Lucas, B.; Omary, M. A.; Larochelle, C. L.; Patterson, H. H. *J. Solid State Chem.* **2002**, *168*, 267.

compared to $In[M(CN)_2]_3$ since they likely hinder motion, especially transverse vibrations of the cyanides. The possible mechanism of PTE and NTE appears to be similar to that postulated for $Ag_3[Co(CN)_6]$. The present findings suggest that flexible d^{10} cyanometallate coordination polymers that do not display significant metallophilicity should be examined for potentially colossal thermal expansion. Such structures may be generated, for example, by increasing cation and/or counterion size (thereby increasing the metal−metal distance and reducing the magnitude of interaction) or by incorporating building blocks that rarely show metallophilicity, such as $Cu(CN)_2^-$. We are presently investigating these avenues.

Acknowledgment. This research is supported by the Natural Sciences and Engineering Research Council of Canada (NSERC). We thank Dr. J. Lefebvre for providing the $KNi[Au(CN)_2]_3$ sample.

Supporting Information Available: Lattice parameters, thermal expansion coefficients, volumes, plots of the lattice parameters as a function of temperature, a sample powder pattern simulation for $In[Au(CN)_2]_3$, and CIF files for $KCd[Au(CN)_2]_3$ at 100, 205, 295, and 395 K. This material is available free of charge via the Internet at http://pubs.acs.org.

JA809631R